Journal of Engineering and Sustainable Development
http://jeasd.uomustansiriyah.edu.iq/index.php
https://doi.org/10.31272/jeasd.25.6.8

Vol. 25, No. 06, November 2021
ISSN 2520-0917

INVESTIGATION OF SINGLE-PHASE FLOW CHARACTERISTICS IN A STAGGER PIN-FINS COMPLEX GEOMETRY

R. Shakir

Petroleum and Gas Engineering Department, College of Engineering, University of Thi-Qar, Iraq.

Published 1/11/2021 ***Accepted in revised form 19/3/2021*** ***Revised 1/11/2021***

Abstract: The cooling equipment project must use electrical and electronic equipment because of the need to remove the heat generated by this equipment. Investigation; R-113 single-phase flow heat transfer; (50 x 50 mm2) cross-section and (5 mm) height; used in a series of stagger-square micro-pin fins. Inlet temperature of (25 °C); (6) Mass flow rate at this temperature, the recommended range is (0. 0025 -0.01 kg/sec) the inlet and outlet pressures are approximately (1-1.10 bar), and through (25- 225 watts) applied heat. The iterative process is used to obtain the heat flow characteristics, for example; the single-phase heat transfer coefficient is completely laminar flow developing, in this flow, guesses the wall temperature, guess the fluid temperature. The possible mechanism of heat transfer has been discussed.

Keywords: *Stagger pin-fins, a Single-Phase of heat transfer coefficients, estimation liquid temperature, and an estimation wall temperature.*

1. Introduction

Heat transfer research on little and micro-projects has progressed substantially during the last decade. As part of a single-phase to heat transfer effort[1-10]. It has always been the most exciting topic. The complex shape of the pin fin provides. Compared with straight channel heat sinks, the complex shape of the fins provides a larger heat transfer area per unit size, thereby reducing thermal inertia. Animations built on the downstream fins allow mixing between fluids and improve heat flow. Many researchers have reported thermal characteristics. On the thermo-hydraulic characteristics of pin-fins on complex geometries, there are some key parameters, such as porosity, heat sink pin-fins, pin- fins configuration; in-line pin- fins, or any pin-fins, tiny fins, a full-length fin, and fin-length, as well as guide, on pin[11-14]. As a result, in compared to other ancient and innovative approaches such as.[5], on this method has advantages, and the thermal properties can be obtained by guessing. This study is a simulation performed by the Excel software used. Assume steady-state and system pressure is close to the atmosphere. It can be seen that the flow is laminar and is fully developing; iterative procedures are used to simulate the heat transfer process. As far as we know, no previous studies have investigated only the characteristics of heat transfer as predictions. The goal of this study is as follows: First, obtain new heat transfer data for R-113 in a single-phase pin-fin array. Secondly, obtain important parameter trends and explore the possibility of the heat transfer mechanism transfer, the third is to find the guessing accuracy of the previous pin-fin correlation, and the fourth is to reinforce the new heat transfer correlation of R-113 on the single phase of the pin-fin array

**Corresponding Author*: raed-sh@utq.edu.iq ;
shraed904@gmail.com

Nomenclature

A_{cell}	unit cell base area (mm^2)
A_{fin}	fin parameter (-)
A_h	heat area (mm^2)
At	total heat of heat sink (mm^2)
C_p	specific heat capacity (kJ/kg K)
D	dimension (-)
D_h	hydraulic diameter (mm)
H_C	mini-channel high (mm)
L	channel length (mm)
K_A	thermal conductivity ($W/m^2.K$)
Mf	flow mass rate (Kg/sec)
NU	Nussle number (-)
qt	position of heat flux (Kw/m^2)
P	channel perimeter cross-section (mm)
Pr	Prandtl number (-)
Re	Reynolds number (-)
T	temperature (K)
Tf	fluid temperature (K)
Tw	wall temperature (K)
W	channel width (mm)
Wc	mini-channel width (mm)
Wcell	cell width (mm)
Ws	solid-channel width (mm)
Z	flow direction (m)
ς_{sp}	single-phase of heat transfer (Kw/m2.K)
η_{fin}	fin efficiency (%)
β	aspect ratio (-)
Φ	equation parameter (-)
Ψ	equation parameter (-)

2. Theory and Formula

The assessment of the transfer of heat characteristics on heat flow is defined by the build of fluid on wall temperatures for relating to suit pressure to seem to fluid temperature.An analysis model of estimating data is classed in a based on stride.

$$\varsigma_{sp} = \left((q_t/A_t)/\left(T_w - T_f\right)\right) \quad (1)$$

Plate sort heaters are used to mark the boundaries of a test area.While insulated, all four sides of the test section were used; an electrical heater was on the bottom of the test section, and an R-113 liquid was on the top of the test section.Fig.1.It offered a demarcation can simply produce a heat flux see uniform on distribution at solid-fluid interface so various forms of equipment to be wanted on conductivity heat by wall been pressed on the analyses. As a result, a significant temperature change on transverse flow was not shown. Thus, a regulating of wall conduction was effect so depicted as a 2-D array; initial-D was perpendicular to R-113 fluid and second-D parallel to R-113 fluid, heat conduction on equation is

$$\delta^2 T/\delta y^2 + \delta^2 T/\delta z^2 = 0 \quad (2)$$

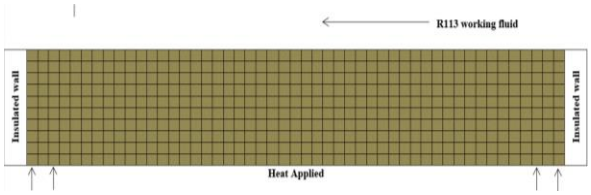

Figure.1. Test Piece Wall Conduction.[15]

Which (y) is a vertical axis to R-113 fluid, and (T) is the temperature of an aluminum wall. The conduction heat equation (2) was obtained by the segmentation of area to square cells cell has (one mm) square; hence, (one mm) cells were utilized in all products listed below. An energy balance is obtained for each cell in Fig.1 by:

$$T_{i,j} = \delta y^2\left(T_{i+1,j} + T_{i-1,j}\right) + \delta z^2\left(T_{i,j+1} + T_{i,j\_1}\right)/2\,(\delta y^2 + \delta z^2) \quad (3)$$

Which (z) and (y) were cell dimensions so eq. (3) and a variance of required to apply a condition on the border; refined was solved to a temperature was the same on each cell. As a result of a prior estimate of an estimating error of (0.001) so the location of the wall temperature was obtained by mediating data as relevant thermocouples, to gain (T_{th}); where was to validate for depth to a plate surface, (L_{th}); and completing an initial-D of conduction heat by the equation below.

$$T_w = T_{th} - (q_t L_{th}/K_A) \quad (4)$$

In which a heat transfer coefficient was obtained by separating up-flow no filed. The cell has a 2-D dimension at the site of a thermocouple, which

was present within a test piece, and fluid temperature may be obtained using the equation below:-

$$T_f = T_{in} + \left(q_t WZ / M_f C_p\right) \quad (5)$$

The following equation was used to estimate the coefficient on single-phase to heat transfer:

$$q_{AE} A_{cell} = \mathrm{U}_{sp}\left(T_w - T_f\right)\left[\left(A_{cell} - A_c\right) + \eta_{fin} A_{fin}\right] \quad (6)$$

Eq. (6) is obtained by employing a normal of an energy balance of unit cell on implicates of single to stagger-pin-fins, in addition, to get an environment on the base-surface to be seen in Fig.1 for left-side on eq. (6) reveals to unit cell has heat input (6). As a result, (cell) denotes a unit cell to the base area.

$$A_{cell} = S_l S_t \quad (7)$$

In which

S_l is the length-wise distance between one central cell and another central cell.

S_t is the width-wise distance between one central cell and another central cell.

A_{fin} is a single pin-fin that has been wetted on its surface area.

$$\mathrm{A}_{fin} = P_{fin} H_{fin} \quad (8)$$

And η_{fin} represents fin efficiency,

$$\eta_{fin} = tanh\left(m_{fin} H_{fin}\right) / m_{fin} H_{fin} \quad (9)$$

In where m_{fin} is fin parameter,

$$m_{fin} = \sqrt{\mathrm{U}_{sp} P_{fin} / K_A \mathrm{A}_c} \quad (10)$$

Which (A_c) is an area on cross-sectional of single stagger-pin-fins

$$\mathrm{A}_c = W_{fin} L_{fin} \quad (11)$$

And (P_{fin}) is the circumference of a single stagger-pin-fin cross-section.,

$$P_{fin} = 2\left(W_{fin} + L_{fin}\right) \quad (12)$$

In where (W_{fin}) is stagger-pin-fin width in (mm);(L_{fin}) is stagger-pin-fins length in (mm) and (H_{fin}) is stagger-pin-fins height in (mm). A guess of wall temperature (T_{wp}) distribution along a stagger- pin-fins channel is computed.

$$T_{WE} = T_{in} + q_{AE} WZ / M_l C_p + A_{cell} q_{AE} / \left[\left(A_{cell} - A_c\right) + \eta_{fin} A_{fin}\right] \mathrm{U}_{sp} \quad (13)$$

Prandtls number is determined by the hydraulic diameter of stagger-pin-fins channel, as shown below: Where:

$$P_r = \frac{C_p \, \mu_f}{k_f} \quad (14)$$

The Reynolds number can be computed by-

$$R_e = \rho_f V D_h / \mu_f \quad (15)$$

In cases when a hydraulic diameter of a stagger-pin-fins channel for heat transfer study is obtained,

$$D_h = \frac{4 \, . \, A_c}{P_{fin}} \quad (16)$$

So just 3-sides of stagger- pin-fins had heated on investigation work, a way employed as in [8]. Is chosen here on a scientific theory to Nussle number to single-phase at R-113 based on a literature to apply it all 4-sides to staggered-pin-fins being heated may be produced by:

$$NU_{x,3} = NU_{x,4} \frac{NU_{fd,3}}{NU_{fd,4}} \quad (17)$$

In where $\mathrm{NU}_{x,4}$, $\mathrm{NU}_{fd,3}$, and $\mathrm{NU}_{fd,4}$, were computed to be obtained respectively, as in[16]. For geometry on boundary conditions had considered. A friction factor had to be obtained as in [16].

$$f_{laminar} R_e = 24(1 - 1.3553 + 1.946\beta^2 - 1.7012\beta^3 + 0.95641\beta^4 - 0.2537\beta^5) \quad (18)$$

A pressure drop (ΔP) had to be obtained for according of method to the eq. (19). In where (β) is a square channel's aspect ratio, and to laminar is a friction factor's Fanning.

$$\Delta P = 2 \, f_{laminar} R_e \, \rho_l V^2 \frac{L}{D_h} \quad (19)$$

3. Prediction Setup

The rig is made up of three main parts: a flow loop system, a test piece made of aluminum stagger-pin-fins with unusual geometry, and an aluminum test section

3.1. Flow Loop

In Figure 2, Rig has a plan for a modern mechanism. The process has a loop structure, as shown below. Since the rig was running a single-phase test sequence, the R-113 liquid was degassed under the high-temperature test sequence for nearly an hour and a half to force the dissolved gas to escape into the atmosphere. At the top of the preheater, the vent valve is intermittently unlocked during this period, allowing the dissolved gas to get away go to the environment. Similarly, adjust the test pressure to be close to atmospheric pressure. After degassing the R-113 liquid, draw it into the accumulator through a pump to ensure that no air or bubbles appear in the liquid in the test assembly before the single-phase test sequence. So, the by-pass valve on the essential pipeline can adjust the required mass flow. As an outcome, coarse filters are mainly utilized to prevent huge debris; therefore, finer filters must be utilized during the test. Subsequently, an estimation test is performed by selecting the best R-113 fluid flow rate and inlet temperature (M_f and T_{in}). A coarse filter is used during the test to capture large particles. Before complex geometries, the mass of R-113 was balanced using flow meters, bypass valves and balance regulating valves. For the mass flow rate of the guess test, the controller adjusts the heat supplied to the R-113 liquid passing through the preheater to adapt to the temperature in the stagger-pin fins with complex geometries on aluminium housing. The controller device connects the preheater to the system. At the same time, adjust the heater of the test part to provide the required heat data for the aluminium sample. R-113 circulates in the designed flow loop until the required steady-state conditions are reached. Therefore, this process takes approximately two and a half hours under steady-state settings. It was significant to keep the outlet heater and the metal shell at a consistent temperature. These queries lasted around (47-75) minutes. To protect against system pressures equivalent to ambient pressures, the approach was iterated inside a single phase and all defined readabilities had to be completed prior to delivering heat and resetting the necessary amount consecutively.

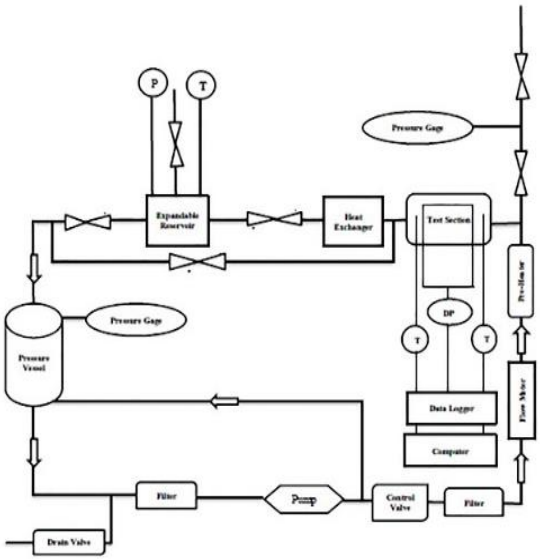

Figure 2. The Flow Loop.[15]

3.2. Test Section

Procedures show Figs. 3 and 4 of an aluminum test segment used in this investigation. An aluminum test section consists of three sections: aluminum housing and an upper cover as a result, aluminum on stagger-pin-fins of complex geometry. If the upper housing, bottom housing, and therefore the body are made of aluminum, the aluminum housing is used. The top housing is made up of complex geometry of aluminum on stagger-pin-fins to complex geometry. It has an entrance and an exit plenum, a pressure port, and a temperature port that is linked to sensors. There

are also two pressure ports, one at the entrance plenum and one at the output plenum.

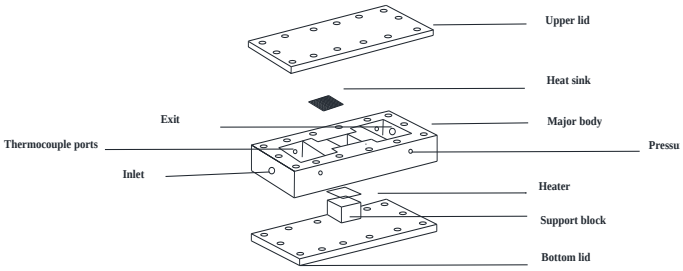

Figure 3. TesHousing. [15]

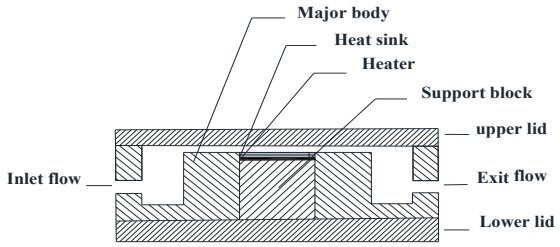

Figure 4. Test Section.[15]

3.3. Test Piece

Figure 5 is an aluminum test piece with a complex geometry of stagger-pin fins; all details have been obtained from this figure; there are then six thermocouple ports, one in each plenum at the inlet and outlet, and four in the aluminum Below the surface, there are stagger-pin fins with complex geometries. Thermocouples are used to determine the temperature of the intake position, the temperature of the outlet position and the temperature of the wall. Therefore, a thermocouple with a probe diameter of (1 mm) is pressed into (2) the hole at the entrance and (2) the hole at the exit. All holes are drilled (8 mm) under the stagger-pin fins on the complex geometric surface The inlet and outlet ends are drilled (20 mm) to the test piece (4). The sheath k-type thermocouple produces these holes, so all thermocouples are measured in extreme water baths and have an accurate (± 1.75 ºC)) to Almost .A slot is used for oon the upper housing to line. Then, each stagger-pin-fins has a footprint of (5 mm) by (5 mm) and a (1 mm) of height .

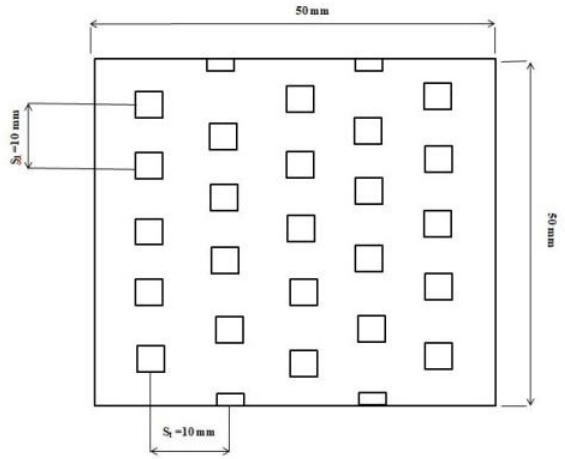

Figure 5. Stagger pin-fins test piece

4. Results and Discussions

Figure 6 illustrates the estimation of the heat transfer coefficient of a single-phase system. For range, single-phase heat transfer and heat range are required. Therefore, the heat transfer coefficients at the entrance and exit positions of the stagger-pin-shaped fins with complex shapes have a single area. It is a laminar development flow, which means that all estimation tests are laminar development flows; therefore, as the mass flux increases, the size of the single-phase laminar flow development area will increase, and the inlet result is much larger than the outlet result. The conduction effect in the wall is an important factor in determining the result. The expansion method of eq. (13) is also included; therefore, all estimation tests for single-phase flow and pressure drop conditions have obtained power relations.

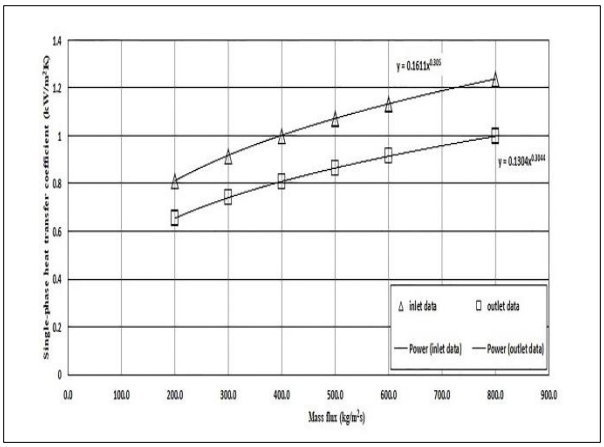

Figure 6. Single-phase of heat transfer versus channel mass flux

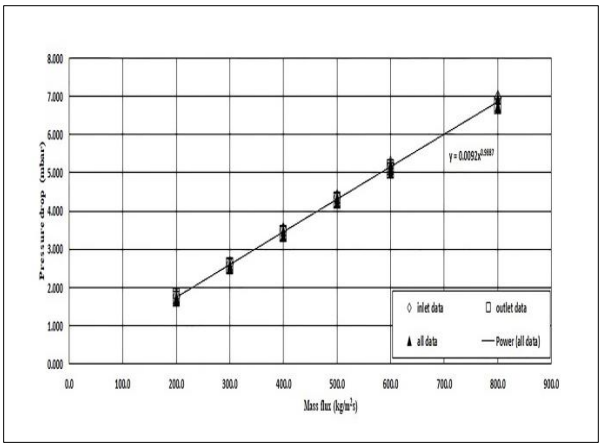

Figure 7. Pressure drop versus channel mass flux

In Figure 7, the estimation of the pressure drop between the inlet pressurization position and the outlet pressurization position is shown to prove that the pressure drop loss and the exit loss occur due to obtaining the flow in the staggered pin fin with complex geometry and obtaining the inlet . All single-phase flow and pressure drop tests produce pressure drop results. As mentioned earlier, the entry loss location and the exit loss location are determined using estimates based on the correlation between Liu and Garimella. As shown in Figure 7, the pressure drop increases as the number of mass flux channels increases. Therefore, the inlet pressure drop is slightly greater than the outlet pressure drop because the pressure drop result depends on the single-phase heat transfer coefficient and fluid characteristics. Subsequently, a power correlation was established for the input and exit results. Finally, it is shown that these estimation results are most consistent with the estimation, theoretical, and empirical correlations.

Fig.8.The results of correlation processing are supplemented.a quantities of single-phase on heat transfer coefficients got to be obtained to each channel to be constituted one zone, laminar developing flows which on heat-transfer coefficient should be obtained from an equation below:-

$$N_U = Ϙ \ln(R_e P_r D_h/L) - \phi \quad (20)$$

The processing set of analyze an uniform of heat flux to be proposed on, (qh), allowed an inlet location and an outlet location of coefficients on heat estimated tests in each heat flux and a mass flux condition.On the other hand, we could be gotted to heat-transfer coefficients tto be employed to use least-squares method on analysis of obtain values of this heat-transfer coefficient is required for a wall conduction type.On eq. (5) Should be used to calculate the temperature of R-113 fluid. Which of these heat-transfer calculations are based on R-113 temperature.This enabled heat flux allocation to be updated by changing the values of the input and exit coefficients for heat transfer.The procedure was repeated till the (Ϙ) and (ϕ) were obtained as the stead case.The iterative data estimate procedure, exemplified in Fig.8, yields the estimation of heat transfer correlation coefficients on eq. (20), (, as 1.9143), and the index (, as 2.9804). Finally, these results show that there is a new correlation between the

estimation of an outlet and an inlet of coefficients in single-phase heat transfer and the hydraulic diameter, the Reynolds number, the Prandtl number, and the distance from the inlet aluminium on the complex geometry of stagger-pin-fins of a heat sink.

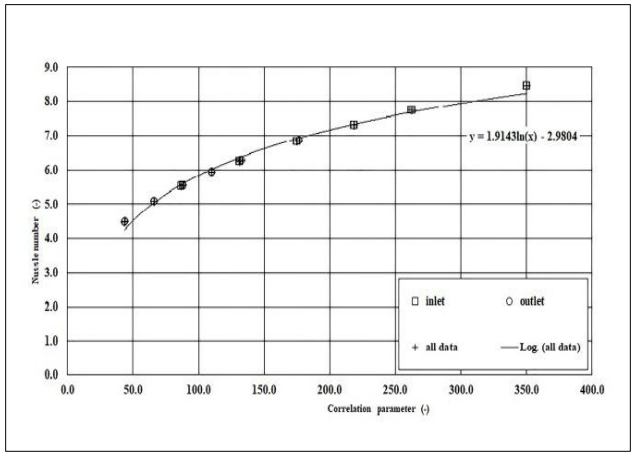

Figure 8. Nussle number versus correlation

5. Conclusions

This is an essential study to identify an inlet and an exit of single-phase for coefficients of heat transfer, and later other results were extensively on pathways with my estimation results. It is encouraging to see that there are no significant discrepancies amongst the outcomes. This inquiry can lead to the following conclusions:

1. In estimation experiments, one zone laminar developing flows were used ;
2. R-113 a liquid property was obtained by estimating R-113 a liquid temperature;
3. During the test series, the highest R-113 a liquid temperature was (32.224 ^{o}C); laminar developing zone, using input data, a result that is bigger than the outlet data result for the test series.
4. The walls are very effectively insulated due to the aluminium test piece; adiabatically was recommended.
5. During a test series, a high fluid temperature is attained with a low mass flow rate.

Acknowledgements

I'd want to express my gratitude to my university colleagues for their assistance in completing this paper.

Conflict of Interest

The authors confirm that the publication causes no conflict of interest

6. References

1. Ravigururajan, T.S. and M.K. Drost, *Single-phase flow thermal performance characteristics of a parallel micro-channel heat exchanger* Journal of Enhanced Heat Transfer, 1999. **6**(1): p. 383-393.
2. Mehendale, S.S., A.M. Jacobi, and R.K. Shah, *Fluid Flow and Heat Transfer at Micro- and Meso-Scales With Application to Heat Exchanger Design.* Applied Mechanics Reviews, 2000. **53**: p. 175-193.
3. Celata, G.P., M. Cumo, and G. Zummo, *Thermal–hydraulic characteristics of single-phase flow in capillary pipes.* Experimental Thermal and Fluid Science, 2004. **28**(2): p. 87-95.
4. Garimella, S.V. and V. Singhal, *Single-Phase Flow and Heat Transport and Pumping Considerations in Microchannel Heat Sinks.* Heat Transfer Engineering, 2004. **25**(1): p. 15-25.
5. Kandlikar, S.G. and W.J. Grande, *Evaluation of Single Phase Flow in Microchannels for High Heat Flux Chip Cooling—Thermohydraulic Performance Enhancement and Fabrication Technology*. Heat Transfer Engineering, 2004. **25**(8): p. 5-16.
6. Li, J., G.P. Peterson, and P. Cheng, *Three-dimensional analysis of heat transfer in a micro-heat sink with single phase flow.*

International Journal of Heat and Mass Transfer, 2004. **47**(19): p. 4215-4231.

7. Owhaib, W. and B. Palm, *Experimental investigation of single-phase convective heat transfer in circular microchannels.* Experimental Thermal and Fluid Science, 2004. **28**(2): p. 105-110.
8. Lee, P.-S., S.V. Garimella, and D. Liu, *Investigation of heat transfer in rectangular microchannels.* International Journal of Heat and Mass Transfer, 2005. **48**(9): p. 1688-1704.
9. Zhang, H.Y., et al., *Single-phase liquid cooled microchannel heat sink for electronic packages.* Applied Thermal Engineering, 2005. **25**(10): p. 1472-1487.
10. Wang, X.-Q., C. Yap, and A.S. Mujumdar, *Effects of Two-Dimensional Roughness in Flow in Microchannels.* Journal of Electronic Packaging, 2004. **127**(3): p. 357-361.
11. Mei, D., et al., *Effect of tip clearance on the heat transfer and pressure drop performance in the micro-reactor with micro-pin–fin arrays at low Reynolds number.* International Journal of Heat and Mass Transfer, 2014. **70**: p. 709-718.
12. Abdoli, A., G. Jimenez, and G.S. Dulikravich, *Thermo-fluid analysis of micro pin-fin array cooling configurations for high heat fluxes with a hot spot.* International Journal of Thermal Sciences, 2015. **90**: p. 290-297.
13. Wang, Y., et al., *Local heat transfer in a microchannel with a pin fin—experimental issues and methods to mitigate.* International Journal of Heat and Mass Transfer, 2017. **106**: p. 1191-1204.
14. Yu, X., et al., *An investigation of convective heat transfer in microchannel with Piranha Pin Fin.* International Journal of Heat and Mass Transfer, 2016. **103**: p. 1125-1132.
15. Lee, P.C. and C. Pan, *Boiling heat transfer and two-phase flow of water in a single shallow microchannel with a uniform or diverging cross section.* Journal of Micromechanics and Microengineering, 2007. **18**(2): p. 025005.
16. London, R.K.S.A.L., *Laminar Flow Forced Convection in Ducts*. 1 ed. 1978, New York: Academic Press. 492.